MAJOR ARTICLE

Rotavirus Induces a Biphasic Enterotoxic and Cytotoxic Response in Human-Derived Intestinal Enterocytes, Which Is Inhibited by Human Immunoglobulins

Giulio De Marco,[1] Ileana Bracale,[1] Vittoria Buccigrossi,[1] Eugenia Bruzzese,[1] Roberto Berni Canani,[1] Gaetano Polito,[1] Franco Maria Ruggeri,[2] and Alfredo Guarino[1]

[1]Department of Pediatrics, University Federico II of Naples, Naples, and [2]Department of Veterinary Public Health and Food Safety, Istituto Superiore di Sanità, Rome, Italy

The mechanisms of diarrhea due to rotavirus infection in humans are not fully understood; no specific therapy is available, but orally administered human serum immunoglobulins are effective in blocking stool output. We aimed to investigate the effect of rotavirus on ion transport and the role of NSP4 in human-derived enterocytes, and to test the efficacy of human serum immunoglobulin in a model of rotavirus infection. Soon after infection, rotavirus induces active chloride secretion in enterocytes. This effect is evident before viral replication leads to cell damage and correlates with NSP4 production. Inhibition of NSP4 prevents the early secretory phase but not cell damage. Incubation with human serum immunoglobulin blocks both ion secretion and cell damage. Rotavirus exerts an early NSP4-dependent ion secretion and subsequent tissue damage. The combined enterotoxic and cytotoxic effects may be responsible for the increased severity of diarrhea due to rotavirus infection, and both are counteracted by human serum immunoglobulin.

Acute gastroenteritis is a major cause of pediatric mortality in developing countries and morbidity in more-developed areas, and rotavirus is the most frequent etiologic agent of gastroenteritis in children [1, 2]. Despite the social and medical costs related to rotavirus gastroenteritis, no specific therapy is currently available. Much effort has been put into the development of a safe and effective vaccine, and currently, 2 different vaccines are available [3, 4].

Rotavirus gastroenteritis is more severe than that caused by other common pathogens, but the reasons for such increased severity are not fully understood [5]. Rotavirus infects mature enterocytes of small intestinal villi, inducing a wide array of functional and structural damages [6, 7]. Several lines of evidence suggest that the destruction of enterocytes and malabsorption cannot completely explain the pathogenesis of rotavirus infection [8–11]. Moreover, early watery diarrhea occurs prior to the detection of villous blunting and other histological changes [11–14]. More recently, studies from animal models led to the identification of novel mechanisms responsible for intestinal secretion during rotavirus infection. Rotavirus-infected cells release a nonstructural protein encoded by the virus, called NSP4, which is able to stimulate age-related and calcium-dependent chloride secretion in mice [15, 16]. However, a complete demonstration of the sequence of events taking place during rotavirus infection and leading to diarrhea is still lacking.

NSP4 is a glycoprotein that interacts with the viral

capsid during rotavirus morphogenesis [17]. Viral sequencing demonstrated high variability, which allowed the definition of 5 NSP4 genetic groups. However, genetic sequencing of NSP4 demonstrated that the variability is mainly located to the C-terminal region of the peptide, between amino acids 110 and 140 in viruses from different species and strains, and this region is important in the virulence of rotavirus [18, 19]. Despite of the importance of NSP4 in the pathophysiology of rotavirus diarrhea in animal models, attempts to detect NSP4 in human-derived models have not been successful, and its role in human disease remains to be elucidated [20].

Rotavirus infects Caco-2 cells, a human intestinal epithelial cell line, and induces a cytotoxic effect with cell lysis and loss of tissue integrity [21]. We previously demonstrated that human serum immunoglobulins (Igs) counteract rotaviral infection in Caco-2 cells, reducing cell damage through a direct anti-rotavirus action [22]. The clinical use of enterally administered Igs was proposed for severe and protracted rotaviral diarrhea [23]. Subsequently, Igs efficacy was shown in children with acute rotaviral diarrhea and in human immunodeficiency virus–infected children [24, 25]. Intriguingly, the effect of Igs was remarkably evident in the very early phases of the disease [24].

In the present study, we investigated the direct effects of rotavirus on transepithelial ion transport, and we were able to set up a model of rotaviral diarrhea in vitro, to investigate the role of NSP4. Finally we tested the efficacy of human serum Igs in this model of rotavirus infection in vitro.

MATERIALS AND METHODS

Study design. The study was performed to clarify the sequence of events taking place at the level of the enterocyte that are potentially responsible for diarrhea after rotavirus infection. In the first part of the study, with use of the Ussing chamber system, we addressed the effect of rotavirus on ion transport and cell viability, namely the capacity of rotavirus to induce chloride secretion and cell damage. Because Ca^{2+} is reported to play a key role in rotavirus infection, we investigated the involvement of Ca^{2+} in the electrical effects induced by rotavirus. Subsequently, we investigated the mechanism of enterotoxicity. Because NSP4 was recognized to act as an enterotoxin, we performed experiments to detect this peptide in rotavirus-infected cells. Finally, neutralization experiments were performed with human serum Igs and with specific anti-NSP4 antibodies.

Cell culture. Caco-2 cells were obtained from the American Type Culture Collection. Cells were grown in high glucose Dulbecco's modified eagle medium with 10% fetal calf serum, 1% nonessential amino acids, 50 mU/mL penicillin, and 50 mg/mL streptomycin, as described elsewhere [26]. Caco-2 cells were grown for 15–18 days after confluence on nontransparent polycarbonate Transwell filters (pore size, 0.4 μM) (Costar Italia). All studies were performed at passages 25–40.

Virus strain and infection protocol. The simian rotavirus strain SA11 is well characterized and is able to replicate to high titers in Caco-2 cells [27, 28]. Virus activation and cell infections were performed in differentiated Caco-2 cells as reported elsewhere [22]. Briefly, the virus was activated with 20 μg/mL trypsin for 30 min at 37°C. Confluent monolayers of Caco-2 cells were washed twice and incubated overnight in fetal calf serum–free medium before virus infection. Viral suspension was added to the apical side of the cell monolayer. After 60 min of incubation at 37°C, the cells were rinsed 3 times and incubated in fetal calf serum–free medium for the established times after infection. The time after infection was started after removal of the excess viral particles. Viral load was determined by plaque forming unit (PFU) assay with MA104 cells, as described elsewhere [29].

Ion transport studies. Ion transport studies were performed in an Ussing chamber model, as reported elsewhere [26]. Briefly, cells were grown in monolayers on uncoated polycarbonate transwell filters. The filter area was 4.9 cm^2. Each filter was mounted in the chamber (WPI) as a flat sheet between the mucosal and the serosal compartments. Each compartment contained 5 mL of Ringer's solution with the following composition: NaCl, 114 mmol/L; KCl, 5 mmol/L; Na_2HPO_4, 1.65 mmol/L; NaH_2PO_4, 0.3 mmol/L; $CaCl_2$, 1.25 mmol/L; $MgCl_2$, 1.1 mmol/L; $NaHCO_3$, 25 mmol/L; and glucose, 10 mmol/L. This solution was constantly gassed with 5% CO_2, 95% O_2 and maintained at 37°C through a thermostat-regulated circulating pump.

Infection with rotavirus was performed with 5 PFUs of virus per cell. The following electrical parameters were measured at different time points after infection, as described elsewhere [30]: transepithelial potential difference (*PD*), short-circuit current (I_{sc}), and tissue ionic conductance (*G*). I_{sc} is expressed as microamperes per square centimeter (μA/cm^2), *G* is expressed as millisiemens per square centimeter (mS/cm^2), and *PD* is expressed as millivolts (mV). Cell viability was evaluated at the end of each experiment by the absence of significant loss in *G* (<20% vs the baseline value) and by measuring the electrical response to the serosal addition of theophylline (5 mmol/L). Cells were considered to be viable and the experiment was considered to be reliable when an I_{sc} increase >5.0 μA/cm^2 was observed after theophylline addition.

To investigate the role of Cl^- in the electrical response, SO_4^{2-} was substituted for Cl^- at an equimolar concentration. We also used the Cl^- channel inhibitor 5-nitro-2–3-(3-phenylpropyl-amino) benzoic acid (NPPB) as described elsewhere [31]. Cells were incubated with NPPB (100 nmol/L) for 30 min before being mounted in Ussing chambers.

In experiments investigating the role of Ca^{2+}, a modified

Ringer's solution was used, with Mg^{2+} substituted for Ca^{2+} at equimolar concentration, to bathe the mucosal side of the filter. The modified Ringer's solution had the following composition: Na_2HPO_4, 1.65 mmol/L; NaH_2PO_4, 0.3 mmol/L; $NaHCO_3$, 25 mmol/L; NaCl, 53 mmol/L; KCl, 5 mmol/L; Na_2SO_4, 30.5 mmol/L; $MgCl_2$, 2.35 mmol/L; glucose, 10 mmol/L; and mannitol, 30.5 mmol/L. In addition, we used the membrane-permeant Ca^{2+} chelator 1,2-bis(2-aminophenoxy)ethane N,N,N',N'-tetraacetic acid/acetoxymethyl ester (BAPTA/AM), as reported elsewhere [31]. Cells were pretreated with 20 mmol/L BAPTA/AM on both the mucosal and serosal sides, 30 min before being mounted in Ussing chambers. To further investigate the role of Ca^{2+}, we used Bay K8644 as a Ca^{2+} inhibitor; we added 1 μmol/L of Bay K8644 20 min before mounting filters in Ussing chambers [32]. This compound acts as a specific agonist of L-type Ca^{2+} channels, causing depletion of intracellular Ca^{2+} stores [33].

Transepithelial resistance measurements. Transepithelial resistance of cell monolayers grown on filters was measured using a Millicel-ERS resistance monitoring apparatus (Millipore). The net resistance was calculated by subtracting the background from the actual value and multiplying the value obtained by the area of the filter (4.9 cm^2). The resistance was expressed in ohms/cm^2. Transepithelial resistance was measured at 1 h intervals for the first 6 h after infection, then at 6 h intervals for the first 24 h, and subsequently every 12 h for 3 days.

Chamber fluids and immunoprecipitation studies. Rotavirus-infected and noninfected cells and chamber fluids were separately collected at different time points after infection. Chamber fluids were filtered through a 0.45-μm Millipore membrane to get rid of cell debris. For experiments in Ussing chambers, 500-μL aliquots of chamber fluids were collected and normalized by protein content.

Cells were lysed by 3 cycles of freezing-thawing, then centrifuged at 10,000 g for 3 min, and pellets were discarded. One mL of the supernatant was diluted in 1 mL of 2$\times$ radioimmunoprecipitation assay buffer (1% sodium deoxycholate, 2% NP-40, 300 mmol/L NaCl, 100 mmol/L Tris pH 7.5, 0.2% sodium dodecyl sulfate, 1 μg/mL aprotinin, 0.5 μg/mL leupeptin, 0.7 μg/mL pepstatin A, and 100 μg/mL phenylmethylsulfonyl fluoride). Immunoprecipitation was performed with 20 μL of rabbit polyclonal anti-NSP4$_{fl}$ antibody for 2 h at 4°C. Subsequently, 50 μL protein-A sepharose were added for 1 h at 4°C. Protein-A sepharose beads were centrifuged at 10,000 g for 30 s, the supernatant was removed, and the beads were then washed 5 times with 1 mL of 1$\times$ radioimmunoprecipitation assay buffer. The beads were again centrifuged, and 100 μL of 2$\times$ radioimmunoprecipitation assay buffer was added to each sample, which were then incubated for 30 min at 37°C. The supernatants were separated by 14% sodium dodecyl sulfate–polyacrylamide gel electrophoresis and were electrotrans-

ferred to nitrocellulose membranes ($\times$2). The membranes were blotted with a different anti-NSP4 antibody (anti-NSP4$_{114-135}$) (1:1000) and with horseradish peroxidase-conjugated goat anti-rabbit IgG. Antibody-specific proteins were visualized by chemiluminescence (Pierce), followed by exposure with Kodak X-Omat film.

Neutralization experiments. After rotavirus infection, Caco-2 cells were incubated with either human serum immunoglobulin preparation (1:5000) or both anti-NSP4 antibodies (1:1000). Both human Igs and anti-NSP4 antibodies were added 1 h after infection to both rotavirus infected and noninfected cells. To investigate the effect of neutralization experiments on ion secretion, we measured I_{sc} modification at 2 h after infection as an outcome parameter, because this was the time point when the maximal enterotoxic rotavirus effect was evident. To investigate the effect of neutralization experiments on cell damage, we measured transepithelial resistance modification at 36 h after infection as an outcome parameter, because this was the time point when the maximal cytotoxic rotavirus effect was evident.

Data collection and statistical analysis. All experiments on ion transport involving the Ussing chamber system and transepithelial resistance measurements were performed by ≥1 operator, whereas data recording, collection, and analysis were blindly performed by a different scientist. Similarly, the results of all other experiments were all blindly analyzed by a scientist other than the one who performed the experiments.

All experiments were performed in triplicate and repeated at least 3 times. Numerical data are expressed as mean values ± standard error of the mean. Data were analyzed using the 2-tailed student's t test.

Antibodies and reagents. All reagents were obtained from Sigma if not otherwise stated. Human serum Igs were obtained from a single commercially available batch for intravenous use, with the following specific neutralizing titers: Rotavirus strain Wa (serotype 1), 1:800; strain DS-1 (serotype 2), 1:1600; strain Price (serotype 3), 1:3200; strain ST-3 (serotype 4), 1:1600. Specific titers were determined as reported elsewhere [24]. Two different anti-NSP4 antibodies were used. One was a rabbit polyclonal antibody raised against a full length form of NSP4 (anti-NSP4$_{fl}$) and was kindly supplied by L. Svensson (University of Linköping, Sweden). The second one was a gift from A. W. C. Einerhand (Erasmus MC-Sophia Children's Hospital, Rotterdam, the Netherlands) and was also a rabbit polyclonal antibody raised against amino acids 114–135 of NSP4 from SA11 strain (anti-NSP4$_{114-135}$) [11].
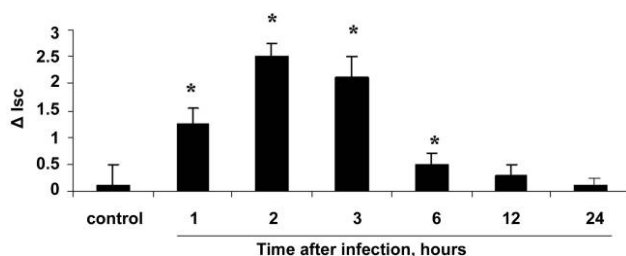
RESULTS

Rotavirus infection induces an early chloride secretion, which precedes tissue damage, in Caco-2 cells. Caco-2 cells infected with rotavirus and mounted in Ussing chambers, showed an

increase in I_{sc}, compared with noninfected cells, which is consistent with anion secretion (figure 1). The increase in I_{sc} was statistically significant at 1 h after infection, reaching a peak after 2 h and then slowly decreasing. At 12 h after infection, electrical evidence of active ion secretion was no longer detected (figure 1). The secretory effect observed in rotavirus-infected cells showed a common pattern with a progressive increase in I_{sc}, which is consistent with a persistent secretory tone.
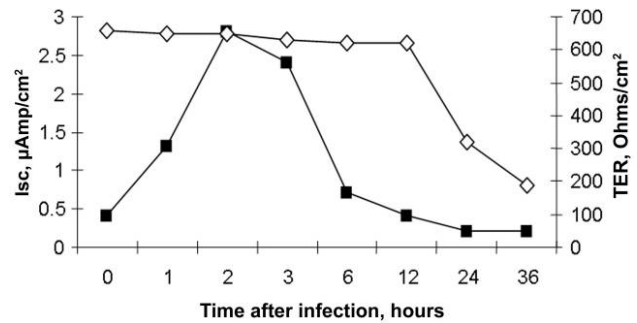
To make sure that the electrical effect was dependent on anion secretion rather than cation absorption, experiments were performed using Cl^--free Ringer's solution at 2 h after infection, this being the time point corresponding to the maximal effect on I_{sc}. Without Cl^-, the electrical effect was virtually abolished (ΔI_{sc}, 0.5 ± 0.5 vs 2.8 ± 0.9 with normal Ringer's solution; $P < .05$). To investigate the role of Cl^- in greater detail, we measured I_{sc} modification in the presence of the Cl^- channel inhibitor NPPB. NPPB completely inhibited the secretory effect of rotavirus (ΔI_{sc}, 0.3 ± 0.3 vs 2.8 ± 0.9 with normal Ringer's solution; $P < .05$). Thus, the effect of rotavirus on I_{sc} was entirely attributable to transepithelial Cl^- secretion.

Time course of the enterotoxic and cytotoxic effects in rotavirus-infected cells. We analyzed together the time course of the effects on ion secretion (reflected by I_{sc}) and on tissue integrity (reflected by transepithelial resistance) (figure 2). Transepithelial resistance did not change in the first few hours after infection. Subsequently, after switching off secretion, starting from 24 h after infection, the cytotoxic effect of the virus became evident, as demonstrated by the decrease in transepithelial resistance (figure 2). These electrical modifications account for a sequence of distinct enterotoxic and cytotoxic mechanisms of rotaviral diarrhea.

Role of calcium in rotavirus-mediated secretion. Rotavirus infection in calcium-free Ringer's solution failed to demonstrated significant ion secretion (ΔI_{sc}, 0.6 ± 0.4 vs 2.8 ± 0.9 with normal Ringer's solution; $P < .05$). Preincubation of cells with both the calcium chelator BAPTA as well as the L-type
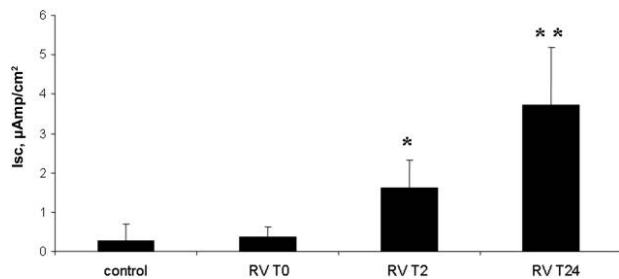

Figure 2. Sequential electrical modification induced by rotavirus in Caco-2 cells. Rotavirus stimulates ion secretion in the early phases of infection, as demonstrated by an increase in short circuit current (I_{sc}) (*black squares*). At the same time points after infection, tissue integrity remains preserved, with transepithelial resistance (TER) (*white diamonds*) remaining unaffected. At later time points, ion secretion is no longer evident, whereas rotavirus begins to damage epithelial integrity, as demonstrated by decrease in TER.

calcium channel inhibitor Bay K8644 was able to block rotavirus-induced secretion (ΔI_{sc}, 0.4 ± 0.2 and 0.5 ± 0.2, respectively; $P < .05$, compared with standard Ringer's solution). This suggests that the secretory effect of rotavirus is Ca^{2+} dependent. In addition, specific inhibition of L-type Ca^{2+} channels completely blocked the electrical effects exerted by rotavirus, suggesting that a major role in ion secretion is played by these type of channels. This set of experiments was performed at 2 h after infection, because this time point corresponded to the maximal effect on I_{sc}.

Dependency on the viral load of rotavirus-mediated secretion. We tested the effects of increasing loads of rotavirus on ion secretion. Chloride secretion was detected after infection with 1 PFU/cell (ΔI_{sc}, 1.05 ± 0.56) and linearly increased with infection with 5 PFU/cell (ΔI_{sc}, 2.8 ± 0.95; $P < .01$, compared with 1 PFU/cell) and 25 PFU/cell (ΔI_{sc}, 4.22 ± 2.25; $P < .05$, compared with 5 PFU/cell, and $P < .01$, compared with 1 PFU/cell). No further increase was observed at 50 PFU/cell, which indicated a saturation pattern. In all other characterization experiments, a single dose of 5 PFU/cell was used.

Chamber fluids from rotavirus-infected cells stimulate ion secretion in noninfected cells. We investigated the presence of enterotoxic moieties by adding aliquots of chamber fluids, obtained from rotavirus-infected cells at different times after infection, to the apical compartment of noninfected Caco-2 cells (figure 3). Their effect was compared with that of chamber fluids from noninfected enterocytes and from cells challenged with rotavirus but in which rotavirus was neither activated with trypsin nor allowed enough time to enter the cell. I_{sc} was measured for 30 min. Chamber fluid from cells collected at 2 h after infection was able to induce ion secretion in noninfected cells (figure 3). The effect was further enhanced with the fluid collected at 24 h after infection. No electrical effect was ob-

Figure 1. Short circuit current (I_{sc}) modifications in rotavirus-infected Caco-2 cells. Rotavirus is able to induce a time-dependent I_{sc} increase in enterocytes, which is consistent with anion secretion. I_{sc} increase is evident at 1 h after infection, peaks at 2 h after infection, and then slowly decreases. Data are mean values ± standard deviation of at least 5 experiments. *$P < .05$.

Figure 3. Enterotoxic effect of chamber fluids from rotavirus (RV)–infected cells. We investigated the presence of enterotoxic moieties released by RV-infected cells. Chamber fluids of RV-infected cells were added to the apical compartment of noninfected enterocytes in the Ussing chamber system. No secretory response was observed with chamber fluids from control cells and from cells in which RV had not been allowed enough time to efficiently infect (T0). In contrast, chamber fluids from cells at 2 (T2) and 24 (T24) h after infection were able to stimulate ion secretion in noninfected Caco-2 cells. $*P < .05$, compared with control; $**P < .01$, compared with control. I_{sc}, short circuit current.

served when rotavirus was not allowed to effectively infect cells (figure 3).

NSP4 production by Caco-2 cells infected with rotavirus. Western blotting with lysates from cells at different time points after infection showed NSP4 at 6 h after infection, and a stronger signal was evident at 24 h after infection (figure 4). Immunoprecipitation experiments were also performed to enhance the sensitivity of detection, and this second set of experiments revealed the presence of NSP4 as early as 1 h after infection. At 24 h after infection, production of NSP4 was further increased (figure 4). We also performed experiments in cell supernatants, but NSP4 was inconsistently detected (data not shown).

Effect of human Igs and anti-NSP4 antibodies on rotavirus cytotoxic and enterotoxic effects. Human Igs were added to rotavirus-infected cells at 1 h after infection, and filters were mounted in Ussing chambers. Incubation with Igs completely abolished rotavirus-induced secretion at all time points (figure 5). In parallel experiments, human Igs were effective in the inhibition of both anion secretion and transepithelial resistance decrease (figure 6). Next, we tested the effect of incubation with specific anti-NSP4 antibodies after rotavirus infection. Anti-NSP4$_{114–135}$ Igs were effective in completely abolishing ion secretion induced by rotavirus infection (figure 6A). No effect was observed for anti-NSP4$_t$. In contrast to human Igs, addition of anti-NSP4$_{114–135}$ and anti-NSP4$_{fl}$ did not affect cell damage induced by rotavirus infection (figure 6B).

DISCUSSION

Rotavirus causes diarrhea through multiple mechanisms. There is convincing evidence, mainly from animal models, of a decreased absorption of electrolytes and glucose/amino acids dur-

ing rotavirus diarrhea [6, 7]. Furthermore, enzymatic activities of the brush border are markedly decreased, and paracellular permeability is increased [6, 7]. Recently, secretory mechanisms have been also described and associated with a viral enterotoxin (NSP4) or with the stimulation of the enteric nervous system [15, 34]. It is a common clinical observation that rotavirus diarrhea occurs with an abrupt onset and massive fluid loss, followed by a milder and more prolonged phase, possibly with transient carbohydrate intolerance and nutrient malabsorption. This clinical pattern is consistent with data from animal models, in which histological changes are preceded by diarrhea induced by rotavirus [11–14].

We set up an experimental model of rotavirus infection in fully differentiated Caco-2 cells, and we were able to detect and characterize a rotavirus-induced enterotoxic effect in enterocytes, in the early phases of infection. The enterotoxic effect consisted of Cl^- secretion with a Ca^{2+}-dependent mechanism. The role of calcium in our model is consistent with previous observations in other models where Ca^{2+} is required for both rotavirus internalization and ion secretion [35]. Following early ion secretion, cell lysis and tissue damage were observed, as demonstrated by the decrease in transepithelial resistance. Thus, in our model of rotavirus infection in vitro, a biphasic response is observed, which parallels the distinct clinical phases. This is the first experimental evidence, to our knowledge, of the sequential secretory and osmotic pathway of diarrhea in a hu-
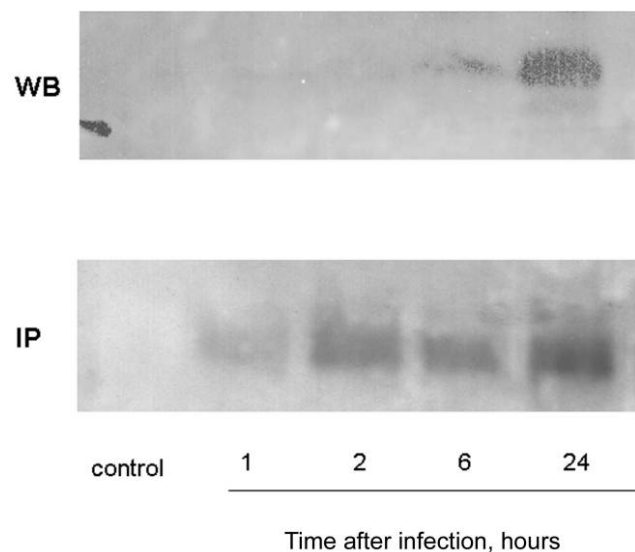
Figure 4. NSP4 detection in Caco-2 enterocytes infected with rotavirus. The demonstration of NSP4 production in Caco-2 cells infected with rotavirus was performed by western blot (WB) in cell lysates (*top panel*) and after immunoprecipitation (IP) (*bottom panel*). WB showed NSP4 from cells at 6 h after infection and a stronger band at 24 h after infection. Increased sensitivity was obtained by immunoprecipitation, allowed the detection of NSP4 starting at 1 h after infection and allowed detection with a stronger signal at later time points.
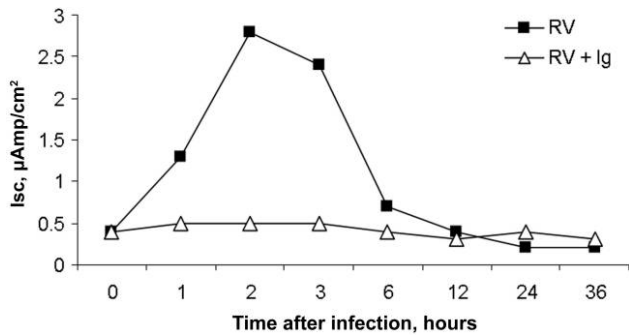
Figure 5. Inhibition of rotavirus (RV)–induced ion secretion by human serum immunoglobulins (Igs). Addition of human serum Igs to RV-infected cells was able to completely abolish the increase in short circuit current (I_{sc}) induced by RV (*white triangles*), compared with RV-infected cells (*black squares*). Inhibition of ion secretion was evident at all time points after infection.

man-derived model. The dual mechanism may well explain the increased severity of rotavirus diarrhea, compared with that induced by other agents.

Because functional evidence of the enterotoxic effect suggested that NSP4 could be involved, we looked for direct proof of its role. The first evidence came from the secretory effect of chamber fluids from rotavirus-infected cells when added to noninfected Caco-2 monolayers. This is the typical effect observed by enterotoxins with a Ca^{2+}-dependent chloride secretion. Direct NSP4 detection led to the demonstration of its presence in the very early phases of infection, coinciding with ion secretion observed in Ussing chambers. The detection of NSP4 in cell lysates, and not in chamber fluids, from infected cells may be ascribed to different experimental conditions in the 2 sets of experiments. A recent study failed to demonstrate ion secretion in rotavirus-infected Caco-2 cells [36]. However, a different rotavirus strain was used, which may account for the production of different nontoxic NSP4 variants [19, 37]. Moreover, in our model, the secretory peak was detected at 2 h after infection, whereas in the other study, events were investigated 4–24 h after infection, when most of ion secretion has already occurred [36].

The more direct evidence pointing to the role of NSP4 was the abrogation of rotavirus-induced ion secretion by anti-NSP4 antibodies. Next, we tested the efficacy of human Igs in this model of rotavirus infection in vitro. Igs are effective in reducing the duration and intensity of diarrhea when orally administered to children with acute rotavirus gastroenteritis [23, 24]. We previously suggested that specific anti-rotavirus antibodies were responsible for the inactivation and clearance of rotavirus [22]. Here, we show that the early secretion induced by rotavirus is completely inhibited by human Igs. This effect is in keeping with the clinical observation that orally administered Igs have a potent therapeutic effect in the very early

phases of rotavirus diarrhea [23]. Thus, Igs are effective on both the enterotoxic and the cytotoxic effects exerted by rotavirus in this in vitro model of infection. A possible explanation would be the presence of anti-NSP4 antibodies in human serum preparations, though this remains to be investigated. A major issue in the study of recently released and potential rotavirus vaccines is the definition of reliable and consistent correlates of protection [38–40]. Our results support the concept that anti-VP4 and VP7 antibodies may be insufficiently correlated to an effective anti-rotavirus condition, because of a potential role of anti-NSP4 Ig.

In conclusion, for the first time, to our knowledge, we directly demonstrated that rotavirus diarrhea has dual secretory and osmotic mechanism, and that the virus strikes the enterocyte with a precise chronological sequence. NSP4 is a central
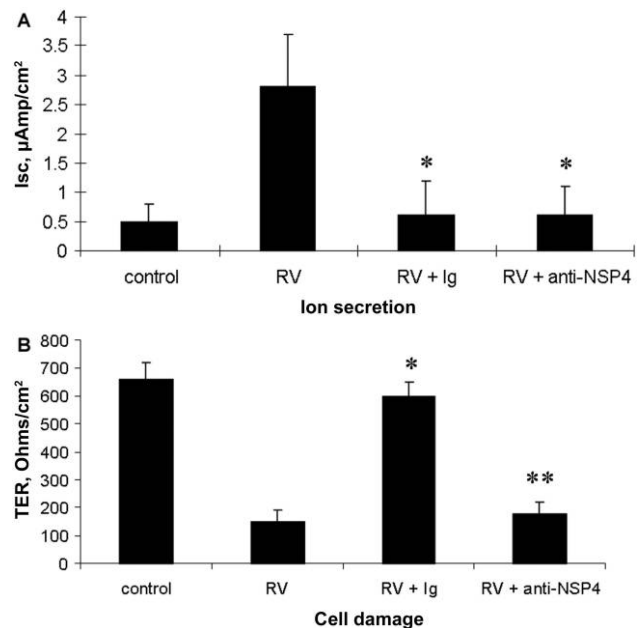
Figure 6. Differential effects of human serum immunoglobulins (Igs) and specific anti-NSP4 antibodies on ion secretion and cell damage induced by rotavirus (RV) in Caco-2 cells. *A,* The effect on ion secretion of human serum Igs and anti-NSP4$_{114-135}$ antibodies was addressed by their addition to RV-infected enterocytes and subsequent I_{sc} measurements. Results were compared with noninfected (control) and RV-infected cells. Both human serum Igs (RV + Ig) and specific anti-NSP4$_{114-135}$ (RV + anti-NSP4) antibodies were able to block RV-induced ion secretion. *$P < .01$, compared with RB-infected, and $P =$ not significant, compared with control. *B,* The effect on cell damage of human serum Igs and anti-NSP4$_{114-135}$ antibodies was addressed by their addition to RV-infected enterocytes and subsequent transepithelial resistance (TER) measurements. Results were compared with noninfected (control) and RV-infected cells. Human serum Igs (RV + Ig) were able to prevent RV-induced cell damage, whereas specific anti-NSP4$_{114-135}$ (RV + anti-NSP4) antibodies did not modify the decreased in TER exerted by RV. *$P < .01$, compared with RB-infected; **$P < .01$, compared with vs RV + Ig, and $P =$ not significant, compared with RV-infected. I_{sc}, short circuit current.

factor in ion secretion in human-derived enterocytes, and human Igs are able to effectively block both phases of diarrhea. This study supports the concept that local immune response and specific anti-NSP4 humoral response should be investigated as candidate correlates of protection in rotavirus diarrhea and of vaccination.

References

1. Kosek M, Bern C, Guerrant RL The global burden of diarrhoeal disease, as estimated from studies published between 1992 and 2000. Bull World Health Organ 2003; 81:197–204.

2. Glass RI, Kilgore PE, Holman RC, et al. The epidemiology of rotavirus diarrhea in the United States: surveillance and estimates of the disease burden. J Infect Dis 1996; 176(Suppl 1):S5-11.

3. Vesikari T, Matson DO, Dennehy P, et al. Safety and efficacy of a pentavalent human-bovine (WC3) reassortant rotavirus vaccine. N Engl J Med 2006; 354:23–33.

4. Ruiz-Palacios GM, Pérez-Schael I, Velazquez FR, et al. Safety and efficacy of an attenuated vaccine against severe rotavirus gastroenteritis. N Engl J Med 2006; 354:11–22.

5. Albano F, Bruzzese E, Bella A, et al. Rotavirus and not age determines gastroenteritis severity in children: a hospital-based study. Eur J Pediatr 2007; 166:241–7.

6. Lundgren O, Svensson L. Pathogenesis of Rotavirus diarrhea. Microbes Infect 2001; 3:1145–56.

7. Estes MK, Kang G, Zeng CQY, Crawford SE, Ciarlet M. Pathogenesis of rotavirus gastroenteritis. 2001. Novartis Found Symp 2001; 238: 82–100.

8. Halls IH, Ruck B, Bishop R, Davidson G. Infantile enteritis; morphogenesis and morphology. J Virol 1975; 16:937–43.

9. Davidson GP, Barnes GL. Structural and functional abnormalities of the small intestine in infants and young children with rotavirus enteritis. Acta Paediatr Scand 1979; 68:181–6.

10. Reynolds D, Hall G, Debney T, Parsons K. Pathology of natural rotavirus infection in clinically normal calves. Res Vet Sci 1985; 38:264–9.

11. Boshuizen JA. Changes in small intestinal homeostasis, morphology, and gene expression during rotavirus infection of infant mice. J Virol 2003; 77:13005–16.

12. Ward LA, Rosen BI, Yuan L, Saif L. Pathogenesis of an attenuated and a virulent strain of group A human rotavirus in neonatal gnotobiotic pigs. J Gen Virol 1996; 77:1431–41.

13. Collins JE, Benfield DA, Duimstra JR. Comparative virulence of two porcine group-A rotavirus isolates in gnotobiotic pigs. Am J Vet Res 1989; 50:827–35.

14. McAdaragh JP, Bergeland ME, Meyer RC, et al. Pathogenesis of rotaviral enteritis in gnotobiotic pigs: a microscopic study. Am J Vet Res 1980; 41: 1572–81.

15. Ball JM, Tian P, Zeng CQ-Y, Morris A, Estes MK. Age-dependent diarrhoea is induced by a viral nonstructural glycoprotein. Science 1996; 272:101–4.

16. Tian P, Hu Y, Shilling WP, Lindsay DA, Eiden J, Estes MK. The nonstructural glycoprotein of rotavirus affects intracellular calcium levels. J Virol 1994; 68:251–7.

17. Au KS, Chan WK, Burns JW, Estes MK. Receptor activity of rotavirus nonstructural glycoprotein NS28. J Virol 1989; 63:4553–62.

18. Tian P, Estes MK, Hu Y, Ball JM, Zeng CQ, Shilling WP. The rotavirus nonstructural glycoprotein NSP4 mobilzes Ca2+ from the endoplasmic reticulum. J Virol 1995; 69:5763–72.

19. Zhang M, Zeng CQ, Dong Y, et al. Mutations in rotavirus nonstructural glycoprotein NSP4 are associated with altered virus virulence. J Virol 1998; 72:3666–72.

20. Lorrot M, Vasseur M. How do the rotavirus NSP4 and bacterial enterotoxins lead differently to diarrhea? Virol J 2007; 4:31.

21. Svensson L, Finlay BB, Buss D, von Bonsdorff CH, Greenberg HB. Symmetric infection of rotavirus on polarized human intestinal epithelial (Caco-2) cells. J Virol 1991; 65:4190–7.

22. Guarino A, Casola A, Bruzzese E, Saini M, Nitsh L, Rubino A. Human serum immunoglobulin counteracts rotaviral infection in Caco-2 cells. Pediatr Res 1996; 40:881–7.

23. Guarino A, Guandalini S, Albano F, Mascia A, De Ritis G, Rubino A. Enteral immunoglobulins for treatment of protracted rotaviral diarrea. Pediatr Infect Dis J 1991; 10:612–4.

24. Guarino A, Berni Canani R, Russo S, et al. Oral immunoglobulins for treatment of acute rotaviral gastroenteritis. Pediatrics 1994; 93:12–6.

25. Guarino A, Albano F, Berni Canani R, Bruzzese E. HIV, fatal rotavirus infection, and treatment options. Lancet 2002; 359:74.

26. Guarino A, Berni Canani R, Casola A, et al. Human intestinal cryptosporidiosis: secretory diarrhea and enterotoxic activity in Caco-2 cells. J Infect Dis 1995; 171:976–83.

27. Estes MK, Graham DY, Gerba CP, Smith EM. Simian rotavirus SA11 replication in cell culture. J Virol 1979; 31:810–5.

28. Kitamoto N, Ramig RF, Matson DO, Estes MK. Comparative growth of different rotavirus strains in different cells (MA 104, Hep G2, Caco-2). Virology 1991; 184:729–37.

29. Wyatt RG, Greenberg HB, James WD, et al. Definition of human rotavirus by plaque reduction assay. Infect Immun 1982; 37:110–5.

30. Field M, Fromm D, Mc Coll I. Ion transport in rabbit ileal mucosa. I. Na+ and Cl− fluxes and short.circuit current. Am J Physiol 1971; 220:1388–98.

31. Guarino A, Bisceglia M, Berni Canani R, et al. Enterotoxic effect of the vacuolating toxin produced by Helicobacter pylori in Caco-2 cells. J Infect Dis 1998; 178:1373–8.

32. Canani RB, Cirillo P, Mallardo G, et al. Effects of HIV-1 Tat protein on ion secretion and cell proliferation in human intestinal epithelial cells. Gastroenterology 2003; 124:368–76.

33. Doggrell S, Hoey A, Brown L. Ion channel modulators as potential positive inotropic compound for treatment of heart failure. Clin Exp Pharmacol Physiol 1994; 21:833–43.

34. Lundgren O, Peregrin AT, Persson K, Kordasti S, Uhnoo I, Svensson L. Role of the enteric nervous system in the fluid and electrolyte secretion of rotavirus diarrhea. Science 2000; 287:491–5.

35. Ruiz MC, Cohen J, Michelangeli F. Role of Ca2+ in the replication and pathogenesis of rotavirus and other viral infections. Cell Calcium 2000; 28:137–49.

36. Catto-Smith AG, Emselle S, Bishop RF. Changes in macromolecular transport appear early in Caco-2 cells infected with a human rotavirus. Scand J Gastroenterol 2008; 43:314–22.

37. Schwartz-Cornil I, Benureau Y, Greenberg H, Hendrickson BA, Cohen J. Heterologous protection induced by the inner capsid proteins of rotavirus requires transcytosis of mucosal immunoglobulins. J Virol 2002; 76:8110–7.

38. Franco MA, Angel J, Greenberg HB. Immunity and correlates of protection for rotavirus vaccines. Vaccine 2006; 24:2718–31.

39. Jiang B, Gentsch JR, Glass RI. The role of serum antibodies in the protection against rotavirus disease: an overview. Clin Infect Dis 2002; 34:1351–61.

40. Hyser JM, Estes MK. Rotavirus vaccines and pathogenesis: 2008. Curr Opin Gastroenterol 2009; 25:36–43.